



HAL
open science

Abnormal operando structural behavior of sodium battery material: influence of dynamic on phase diagram of Na_xFePO_4

Joël Gaubicher, Florent Boucher, Philippe Moreau, Marine Cuisinier, Patrick Soudan, Erik Elkaim, Dominique Guyomard

► To cite this version:

Joël Gaubicher, Florent Boucher, Philippe Moreau, Marine Cuisinier, Patrick Soudan, et al.. Abnormal operando structural behavior of sodium battery material: influence of dynamic on phase diagram of Na_xFePO_4 . *Electrochemistry Communications*, 2013, 10.1016/j.elecom.2013.11.017 . hal-00906676v1

HAL Id: hal-00906676

<https://hal.science/hal-00906676v1>

Submitted on 21 Nov 2013 (v1), last revised 11 Dec 2013 (v2)

HAL is a multi-disciplinary open access archive for the deposit and dissemination of scientific research documents, whether they are published or not. The documents may come from teaching and research institutions in France or abroad, or from public or private research centers.

L'archive ouverte pluridisciplinaire **HAL**, est destinée au dépôt et à la diffusion de documents scientifiques de niveau recherche, publiés ou non, émanant des établissements d'enseignement et de recherche français ou étrangers, des laboratoires publics ou privés.

Abnormal *operando* structural behavior of sodium battery material: influence of dynamic on phase diagram of Na_xFePO_4

J. Gaubicher*^{1,3}, F. Boucher^{1,3}, P. Moreau^{1,3}, M. Cuisinier^{1,3},
P. Soudan^{1,3}, E. Elkaim², and D. Guyomard^{1,3}

¹*Institut des Matériaux Jean Rouxel, UMR 6502, CNRS - Université de Nantes, 2 rue de la Houssinière, B.P.32229, 44322 Nantes cedex France*

²*Synchrotron SOLEIL, 91190 St Aubin, France*

³*Réseau sur le Stockage Electrochimique de l'Energie (RS2E), FR CNRS 3459, France*

Corresponding author: joel.gaubicher@cnrs-in.fr

Abstract

This study conveys striking findings regarding the *operando* structural behavior of the Na/FePO₄ system during a charge and discharge cycle. From Rietveld refinements of synchrotron *operando* X-Ray diffraction data, it appears that the active material presents large, non-stoichiometric domains while undergoing structural phase transformation. The corresponding extended limits of solubility are characterized by continuous variations in the metrics that mirror the entry of Na occupancy values into thermodynamically forbidden regions. A major consequence of this smoothed phase transformation is a significant decrease in the lattice volume mismatch, which could well compensate for the less efficient Na-based systems with respect to SEI and adverse effect of cation size in comparison to Li batteries. Comparison of the lattice volume mismatch on charge and discharge revealed an explanation for the asymmetry of the electrochemical curve.

Keywords: Na-ion battery, NaFePO₄, *operando* XRD, olivine

1. Introduction

Large-scale Na-ion batteries are envisioned as a possible alternative to Li-ion ones as far as availability and environmental issues are concerned. Following the pioneering work of

Delmas [1] this field has shown renewed interest in recent years and is currently inciting ever-expanding research. This is especially the case with regard to improvement of electrolytes [2-3], as well as to the discovery of highly reversible materials having large energy densities [4]. Inspired by the remarkable electrochemical properties of LiFePO₄, the electrochemical and structural study of the olivine NaFePO₄ has shown some singularities [5,6,7,8]. Indeed, based on ex-situ X-ray diffraction (XRD), it was shown that the room temperature phase diagram of Na_xFePO₄ consists of a single phase process between 2/3 < x < 1 [6,8] and a two-phase process between 0 < x < 2/3 [5-8]. In order to gain insight into the actual structural behavior of the material in an operating Na battery, this communication reports results related to *operando* XRD using synchrotron radiation. Based on XRD data of very high quality, it will be shown that dynamics have a striking and crucial impact on the structural response of the material.

2. Experimental

Carbon-coated FePO₄ was derived by electrochemical oxidation of a carbon-coated-LiFePO₄ (LFPC, obtained from UMICORE) based electrode upon potentiostatic equilibration at 4.0V vs. Li⁺/Li⁰ in a LP30-electrolyte (Novolyte). The LFPC electrode was made of 85wt% LFPC, 5wt% PVDF and 10 wt% Carbon-Super-P. The electrode was then extensively washed with DMC and transferred to a Na half cell with NaClO₄-1M in propylene carbonate as the electrolyte. All voltages given in the following text are reported vs. Na⁺/Na⁰.

A fully intercalated NaFePO₄ compound-based electrode was obtained from the FePO₄ one upon discharge to 2V at C/50 and subsequent potentiostatic equilibration at 2V for 24 hours. The final Na composition derived from integration of the charge passed was 0.98. This electrode was finally mounted in the *operando* XRD cell[9] and cycled at 1Na/23h, using a VMP3 potentiostat. Five potentiostatic equilibration periods were applied as follows: on charge at 3.020V for 1h, 3.300V for 1.5h, and 3.295V for 10h, and then on discharge at 2.820V and 2.000V for 1h. The two floating periods at 3.300V and 3.295V were separated by an open-circuit-voltage (OCV) period for 10h.

Operando XRD characterization was conducted at the CRYSTAL beamline of the SOLEIL French synchrotron source ($\lambda = 0.725633 \text{ \AA}$) using a Mar image plate detector in transmission geometry. XRD diagrams were collected up to $2\theta = 33^\circ$ every 10 minutes. Each diagram lasted for 2s. No XRD data was measured during the entire OCV and 2.95V floating periods.

Rietveld analyses were achieved by using the FullprofSuite software in a Pnma metric. Rietveld refinement of Na_xFePO_4 compounds ($x>0.05$), henceforth referred to as $\text{Na}_{\text{RICH}}\text{FePO}_4$, and Na_xFePO_4 compounds ($x\leq 0.05$), henceforth referred to as $\text{Na}_{\text{POOR}}\text{FePO}_4$ were conducted beginning with the structural models for NaFePO_4 [5] and FePO_4 [10] respectively using soft constraint on P-O bonds. During the phase transformation process, approximations had to be made due to structural instabilities when refining all parameters in sequential mode. Therefore, only cell parameters and scale factors were allowed to vary during sequential refinements of phase transformations as soon as the weight fraction of the disappearing compound was below 0.95. In these cases, Na occupancies, atomic coordinates, and profile parameters of both compounds were taken from “reference” refinements. The scan numbers used to get those reference values were scans 151 and 470 for $\text{Na}_{\text{RICH}}\text{FePO}_4$ and $\text{Na}_{\text{POOR}}\text{FePO}_4$ respectively, on charge, and scans 576 and 470 for $\text{Na}_{\text{RICH}}\text{FePO}_4$ and $\text{Na}_{\text{POOR}}\text{FePO}_4$ respectively, on discharge. Thanks to XRD of very high quality, R_{BRAGG} and R_{F} reliability factors were always below 4%, thereby confirming that satisfactory refinements were obtained. Standard deviations for weight fractions (0-1), volumes ($\sim 300\text{\AA}^3$) and Na occupancies (0-1) were below 0.005, 0.3 and 0.01 respectively. The description of the system is thus considered to be highly accurate.

3. Results and discussion

The charge process corresponds to $\Delta x=0.83$ during X-ray exposure (scans 1-237) plus an additional $\Delta x=0.09$ during potentiostatic equilibration at 3.295V (without X-ray exposure). The subsequent discharge (scans 470-662) leads to a slightly lower value $\Delta x=0.72$, the difference being ascribed to kinetic issues (see further down in this section). Due to beam shutdown, the electrochemical experiment was placed in OCV for $\sim 6\text{h}$ at $x=0.74$ on charge. Milestone numbers of XRD scans, which will be discussed in the following, are reported on Fig. 1a. Fig. 1a and the corresponding inset shows the two processes expected for the Na_xFePO_4 system: a single-phase region between roughly $0.6<x<1$ [6,8], and a two-phase process between $0.1<x<0.6$ on charge [5-8]. All these features are consistent with those observed when using a regular Swagelok-type cell [5], thus confirming the reliability of the *operando* XRD cell [9]. Quantification of the effect of dynamics (C/23 rate) on structural aspects was gained from Rietveld refinements in sequential mode. The weight fractions of both $\text{Na}_{\text{RICH}}\text{FePO}_4$ and $\text{Na}_{\text{POOR}}\text{FePO}_4$ as well as their respective Na occupancies are reported

in Fig. 1b. We note that close examination of angular ranges (5-8° and 12-13°) within which superstructure lines were expected [5-6], shows that the latter do not appear under galvanostatic conditions. For this reason, the Pnma unit cell [5] was used to fit XRD data. It is very instructive to note that when the potential reaches the phase transformation plateau (3.07V, scan 121 in Fig. 1a), the Na composition is close to 0.6 from both electrochemistry and Rietveld refinement, which compares well with the composition threshold of 2/3 that is expected in order for the phase transformation to initiate [8]. We noted that even though the phase transformation had already started, according to the potential probe (scan 121), the XRD data did not show the appearance of the Na_{POOR}FePO₄ compounds before scan 145. Due to the fact that the intensity of the Na_{RICH}FePO₄ lines does not vary between scans 121 and 145, whereas (as shown further down) the Na_{RICH}FePO₄ compounds are still reacting, this slight delay cannot be ascribed to inhomogeneities such as those in ref [11]. Instead, we propose that the formation of a low proportion of small, coherent domains of Na_{POOR}FePO₄ compounds should be considered.

Both molar fraction of the two types of compounds, as well as $\tau(\text{Na})$, can be used to determine the degree of deintercalation/intercalation of the Na ions in Na_xFePO₄ (referred to as x_{XRD}), such as in the following:

$$x_{\text{XRD}} = \text{Mol}\%(\text{Na}_{\text{RICH}}\text{FePO}_4) * \tau(\text{Na})_{\text{Na}_{\text{RICH}}\text{FePO}_4} + \text{Mol}\%(\text{Na}_{\text{POOR}}\text{FePO}_4) * \tau(\text{Na})_{\text{Na}_{\text{POOR}}\text{FePO}_4}$$

As described in the experimental section, $\tau(\text{Na})$ had to be fixed to “reference” values when both Na_{RICH}FePO₄ and Na_{POOR}FePO₄ were present. Accordingly, inaccuracies appear in these sections. For this reason, both $\tau(\text{Na})$ and x_{XRD} were plotted with dashed lines in Fig. 1b. Nevertheless, as shown in Fig. 1b, values of x_{XRD} correspond rather well with those of x_{electro} thereby confirming the reliability of the Rietveld refinements.

Fig. 1c shows the variations of the cell volumes on charge and discharge for both Na_{POOR}FePO₄ and Na_{RICH}FePO₄ compounds. Maximum volume and Na composition of Na_{RICH}FePO₄ were $\tau(\text{Na})=0.948(4)$ and $V=318.331(9) \text{ \AA}^3$, as refined on scan 1 ($R_{\text{Bragg}}=1.19\%$ and $R_{\text{F}}=1.01\%$), while for Na_{POOR}FePO₄ minimum ones were $\tau(\text{Na})=0.05(1)$ and $V=275.39(1) \text{ \AA}^3$, as refined on scan 470 ($R_{\text{Bragg}}=1.91\%$ and $R_{\text{F}}=1.30\%$). Surprisingly, although XRD detects structural phase transformation between scans 145-237 on charge and 470-662 on discharge, results of Fig. 1c demonstrate that, simultaneously, lattice volumes vary significantly. We note that (i), given the transmission geometry of the X-ray diffraction processes, these effects cannot be ascribed to sample displacements, and that (ii) no

significant line broadening was measured. With regards to $\text{Na}_{\text{RICH}}\text{FePO}_4$, values of $V(\text{\AA}^3)$ go well below those expected for $\text{Na}_{2/3}\text{FePO}_4$ [8]. Furthermore, Fig. 1b shows that on charge this unexpected volume variation is associated with a continuous decrease of the Na occupancy values down to $\tau(\text{Na})=0.45(1)$ on scan 151, where the composition of the electrode contains ~95/5 of $\text{Na}_{\text{RICH}}\text{FePO}_4$ / $\text{Na}_{\text{POOR}}\text{FePO}_4$ compounds. This decrease was confirmed by non-sequential Rietveld refinement on scan 185 which leads to $\tau(\text{Na})=0.34(1)$ ($R_{\text{Bragg}}=1.61\%$ and $R_{\text{F}}=1.08\%$). Accordingly, we are witnessing the occurrence of vastly extended limits of solubility. These are characterized by a continuous variation of the metric which is mirroring that of the Na occupancy (and hence that of the Fe(III)/Fe(II) ratio). Therefore, arguments such as whether or not a delay between XRD and electrochemical measurements are at play, or such as the occurrence of inhomogeneities between parts of the electrode under and out of the beam, are pointless, since the present findings concern the entry of parameters defining the system ($t(\text{Na})$, $V(\text{\AA}^3)$...) in thermodynamically forbidden regions [8]. This striking result, hitherto unseen in material science, to our knowledge, highlights the fact that the thermodynamic phase diagram of this Na/FePO₄ system, as established by Yamada [8], needs thorough reassessment as far as the operating material is concerned. Indeed, the phase transformation limits are unexpectedly and markedly smoothed out in such a way that the electrochemical insertion/deinsertion of Na ions occurring at the phase front, between domains of $\text{Na}_{\text{POOR}}\text{FePO}_4$ and $\text{Na}_{\text{RICH}}\text{FePO}_4$ compounds, does exhibit a variation of Na composition. A direct and major consequence of this finding lies in the fact that the lattice volume mismatch between the two protagonists of the phase transformation is greatly reduced. As a matter of fact, the integrated volume mismatch over the mol% variation of $\text{Na}_{\text{RICH}}\text{FePO}_4$ compounds during the phase transformation on charge is 19.8\AA^3 , that is to say 30% lower than the value obtained (28.2\AA^3) considering a phase transformation occurring at constant volumes with $V_{\text{Na}_{2/3}\text{FePO}_4}=308.551\text{ A}^3$ from reference [8] and $V_{\text{Na}_{0.05}\text{FePO}_4}=275.39(1)\text{ A}^3$ as refined on scan 237. Considering the fact that significant volume mismatch (>10%) influences the stability of the solid electrolyte interphase (SEI) on cycling, which is one of the detrimental factors governing the cycle life of battery materials [12], it seems that Na active material may have a decisive advantage over Li battery ones (and that this may well compensate for known adverse effects such as those associated with the size of Na^+ and inefficient Na related SEI). This also goes to show that, contrary to the Li case, *operando* behaviors and thermodynamic expectations are strikingly different in the case of Na batteries. For this reason, the oodles of results that have been gathered for Li-ion batteries over the past two decades should not be taken as readily transferable to Na-ion batteries. Additional

instructive information stems from Fig. 1c. Indeed, Rietveld refinements clearly show that the lattice volume behaviors on charge and discharge are asymmetrical both for the $\text{Na}_{\text{RICH}}\text{FePO}_4$ and the $\text{Na}_{\text{POOR}}\text{FePO}_4$ compounds. This is particularly evident during the phase transformation where the volume variation of $\text{Na}_{\text{POOR}}\text{FePO}_4$ compounds is much less pronounced on discharge (Fig. 1c), while that of $\text{Na}_{\text{RICH}}\text{FePO}_4$ ones increases more rapidly than on charge. This is well illustrated in the inset of Fig. 1c that compares two scans of similar composition ($\sim 50/50$), but obtained on charge (scan 201) and on discharge (scan 520). Indeed, hkl lines of $\text{Na}_{\text{POOR}}\text{FePO}_4$ are observed at similar angles in both cases, whereas those of $\text{Na}_{\text{RICH}}\text{FePO}_4$ are clearly shifted to lower angles on scan 520. It appears, therefore, that the lattice volume mismatch should be greater on discharge. For the sake of comparison, a calculation using the same range of molar fractions as previously selected for the charge, shows that volume mismatch does in fact increase to reach 25.5\AA^3 on discharge (that is 22% higher compared to the 19.9\AA^3 found on charge as shown above). Accordingly, a higher thermodynamic potential hysteresis is expected on discharge. This hysteresis should lower the voltage of the potential plateau on discharge, thereby accounting for the much reduced voltage difference (a few mV) observed on discharge between the two electrochemical processes [5-7]. Therefore as proposed by Yamada [8], under current load, kinetic overpotential provides an excess of energy to the system that can consequently, given the small voltage gap, access both the phase transformation and the single phase processes simultaneously. In other words, Na is consumed for both types of solid-state reactions, which may also explain why the phase transformation on discharge lasts until the end of the experiment.

4. Conclusion

Contrary to what has been observed in material science to date, and more particularly in the Li battery field, a structural phase transformation occurring for an operating sodium battery material, namely Na_xFePO_4 , does not proceed at constant composition. Indeed, vastly extended limits of solubility that correspond to thermodynamically forbidden regions have been evidenced simultaneously to variation of phase proportion. Considering the initial FePO_4 material, this striking behavior results in Na batteries having an enormous advantage over Li ones, since their unit cell volume mismatch during phase transformation is greatly reduced. Indeed, as far as cyclability and therefore battery price is concerned, kinetically controlled

structural behavior such as this can clearly compensate for the less efficient Na-related SEI as well as the larger size of Na ions. Lastly, the asymmetry of the electrochemical behavior between charge and discharge is tentatively explained based on the fact that the discharge process corresponds to a 22% higher volume mismatch than the charge process.

In the near future, we anticipate the elucidation of further noteworthy examples regarding the influence of dynamics on the structural behavior of positive and negative electrode materials of the Na battery. The influence of cycling rate is currently being investigated.

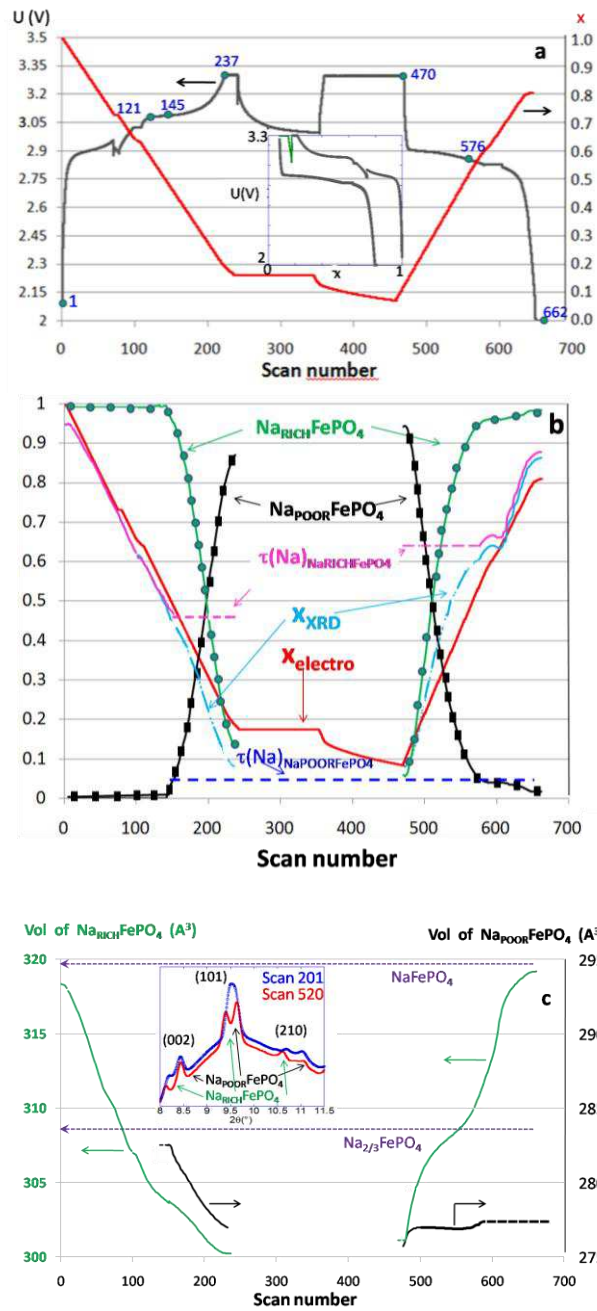


Figure 1: Variation as a function of scan numbers during charge and discharge of (a) potential (inset shows the potential-composition curve), (b) x_{electro} , x_{XRD} (dotted lines correspond to approximations using constant $\tau(\text{Na})=0.05(1)$ for $\text{Na}_{\text{POOR}}\text{FePO}_4$ and $\tau(\text{Na})=0.45(1)$ for $\text{Na}_{\text{RICH}}\text{FePO}_4$), $\tau(\text{Na})$ for $\text{Na}_{\text{POOR}}\text{FePO}_4$, and weight fractions and, (c) lattice volumes (dashed lines correspond to regions where intensities were too low to allow reliable refinements, and dotted lines to volumes of NaFePO_4 and $\text{Na}_{2/3}\text{FePO}_4$ from refs. [5] and [8] respectively); inset shows XRD diagrams corresponding to a similar composition close to 50/50 of $\text{Na}_{\text{POOR}}\text{FePO}_4$ and $\text{Na}_{\text{RICH}}\text{FePO}_4$, but obtained on charge (scan 201) and on discharge (scan 520)

References

- [1] C. Delmas, J.J. Braconnier, C. Fouassier, P. Hagenmuller, *Solid State Ionics* 3 (1981), pp.165.
- [2] C. Vidal-Abarca, P. Lavela, J.L. Tirado, A.V. Chadwick, M. Alfredsson, E. Kelder, *J. Power Sources* 197 (2012), pp.314.
- [3] A. Ponrouch, A. R. Dedryvere, D. Monti, AE. Demet, JMA. Mba, L. Croguennec, C. Masquelier, P. Johansson, MR. Palacin, *Energy and Env. Science* 6 (2013), pp.2361.
- [4] N. Yabuuchi, M. Kajiyama, J. Iwatate, H. Nishikawa, S. Hitomi, R. Okuyama, R. Usui, Y. Yamada, S. Komaba, *Nature Materials* 11 (2012), pp.512.
- [5] P. Moreau, F. Boucher, J. Gaubicher, and D. Guyomard, *Chem. Mat.* 22 (2010), pp.4126.
- [6] P. Moreau, M. Cuisinier, B. Turpin, J. Gaubicher, F. Boucher and D. Guyomard, "Elucidation of the $\text{Na}_{2/3}\text{FePO}_4$ intermediate phase: clues to the insertion process in olivine" 7th International Symposium on Inorganic-Phosphate-Materials (ISIPM7), November 8-11, 2011.
- [7] M. Casas-Cabanas, V.V. Roddatis, D. Saurel, P. Kubiak, J. Carretero-Gonzales, V. Palomares, P. Serras and T. Rojo, *J. Mater. Chem.* 22 (2012), pp.1742.
- [8] J. Lu, S-C. Chung, S.-I. Nishimura, G. Oyama, and A. Yamada, *Chem. Mater.*, DOI:10.1021/cm402617b.
- [9] J.B. Leriche, S.Hamelet, J. Shu, M. Morcrette, C. Masquelier, G. Ouvrard, M. Zerrouki, P. Soudan, S. Belin, E. Elkaïm, & F. Baudelet, *Journal of The Electrochemical Society*, 157 (2010), pp.A606-A610.
- [10] M. Wagemaker, B.L. Ellis, D. Luetzenkirchen-Hecht, F.M. Mulder, and L.F. Nazar, *Chem. Mater.*, 20 (2008), pp.6313.
- [11] G. Ouvrard, M. Zerrouki, P. Soudan, B. Lestriez, C. Masquelier, M. Morcrette, S. Hamelet, S. Belin, A.M. Flank, F. Baudelet, *J. Power Sources* 229 (2013), pp.16.
- [12] X. Lin, J. Park, L. Liu, Y. Lee, A.M. Sastry, and W. Lu, *J. Electrochem. Soc.* 160 (2013), pp.A1701-A1710.